Research Article

MOLECULAR PAIN

Molecular Pain
Volume 15: 1–13

DOI: 10.1177/1744806919871813
journals.sagepub.com/home/mpx
SAGE

2-Bromopalmitate attenuates bone cancer pain via reversing mitochondrial fusion and fission imbalance in spinal astrocytes

Wei Meng[1], Miao-Miao Hao[2], Na Yu[1], Ming-Yue Li[2], Jie-Qiong Ding[1], Bang-Hua Wang[1], Hai-Li Zhu[1], and Min Xie[1]

Abstract

Bone cancer pain is common in patients with advanced cancers as tumors metastasize to bone. Pathogenesis of bone cancer pain is complex and poorly understood which leads to inefficiency of clinical treatment. During pathological pain status, astrocytes are activated and release various inflammatory cytokines, which result in the development of peripheral and central sensitization. As energy factory, mitochondria undergo frequent fusion and fission and play essential role for astrocyte function. 2-bromopalmitate (2-BP) is an inhibitor of protein palmitoylation, and its function on bone cancer pain was unclear. In this article, we aimed to investigate the potential curative effects and mechanisms of 2-BP on bone cancer pain. Bone cancer pain rat model was established through intratibial inoculation of rat mammary gland carcinoma cells (MRMT-1) into the left tibia of Sprague–Dawley female rats. As a result, bone cancer pain rats exhibited bone destruction and sensitive nociceptive behavior. And increased leukocyte infiltration, activation of astrocytes, and imbalance of mitochondrial fission and fusion dynamics were observed in spinal cord of bone cancer pain rats. Intrathecal 2-BP administration significantly attenuated pain behavior of bone cancer pain rats. Meanwhile, 2-BP administration reduced spinal inflammation, reversed spinal mitochondrial fission and fusion dynamic imbalance, and further inhibited spinal mitochondrial apoptosis in bone cancer pain rats. In C6 cell level, 2-BP treatment decreased dynamin-related protein 1 expression and increased optic atrophy 1 expression in a dose-dependent manner and inhibited carbonyl cyanide 3-chlorophenylhydrazone (CCCP)-induced mitochondrial membrane potential change. These data illustrated that 2-BP attenuated bone cancer pain by reversing mitochondrial fusion and fission dynamic imbalance in spinal astrocytes.

Keywords

Bone cancer pain, 2-bromopalmitate, spinal astrocyte, mitochondrial fission and fusion

Date Received: 24 April 2019; revised: 30 May 2019; accepted: 17 June 2019

Introduction

Cancer pain is one of the most common clinical symptoms associated with malignant cancers.[1] Many common malignant tumors, especially breast, prostate, kidney, and lung tumors have a strong predilection metastasize to bones.[2] Tumor cells grown in bone causes bone destruction, woven bone formation, and moderate to severe bone pain which are the common symptoms in the patients.[3] Bone cancer pain (BCP) is usually described as dull in character, constant in presentation, and gradually intensifies to severe incident pain, which debilitates patient's quality of life and functional status.[4] Until now, the complex pathological and molecular mechanisms of BCP result in the poor effectiveness of clinical treatment, and most pharmacological treatments for BCP had undesirable side effects. Accordingly, understanding the mechanisms and improving available agents of BCP is desirable.

[1]Department of Physiology, School of Basic Medical Sciences, Research Center of Basic Medical Sciences, Hubei University of Science and Technology, Xianning, China
[2]School of Pharmacy, Hubei University of Science and Technology, Xianning, China

The first three authors contributed equally to this work.

Corresponding Author:
Min Xie, Hubei University of Science and Technology, No.88 Xianning Avenue, Xianning City, Hubei Province 437100, China.
Email: mmtmrxm@sina.com

Astrocytes are the most abundant cell type widely distributed throughout central nervous system (CNS).[5,6] In CNS, astrocytes are structurally in close association with synapses, contributing to the establishment and reorganization of neuronal circuits and maintenance of synaptic structure.[7] In addition to physiological functions, astrocytes contribute to chronic pain. Research demonstrates that in chronic pain and pain-related injury states, activation of astrocytes usually occurring several days after the injury and much longer lasting.[8] During pathological pain status, activated astrocytes release various inflammatory cytokines, such as interleukin (IL)-1β and tumor necrosis factor-alpha.[9] The production of proinflammatory mediators modulates pain sensitivity, which leads to the development of peripheral and central sensitization, and induction of chronic pain conditions.[10]

Mitochondria play critical roles in energy metabolism, cell survival, and synaptic plasticity.[11] Healthy mitochondria are highly dynamic organelles and undergo frequent fusion and fission in character which is essential for astrocyte function.[12] Furthermore, dynamic balance between fusion and fission is critical for the maintenance of mitochondrial morphology and functions.[13] Fusion is the lengthening of mitochondria by tethering and joining adjacent mitochondria, allowing the exchange of DNA, contents, and metabolites between neighboring mitochondria.[14] Fission involves the constriction and cleavage of mitochondria, enabling the distribution and transport of mitochondria.[15] Mitochondrial fusion and fission are mediated by high molecular weight GTPases proteins including optic atrophy 1 (OPA1) and dynamin-related protein 1 (Drp1). OPA1 is a nuclear dynamin-related GTPase and mediated mitochondrial inter membrane fusion.[16] Drp1 is primarily localized in cytoplasm, translocation of which from cytoplasm to mitochondrial outer membrane (MOM) drives mitochondrial constriction and division.[17] Accumulating evidence suggests that dysregulation of OPA1 and Drp1 is related to the abnormality of neurological function. *Opa1* homozygous mutant mice are lethal in embryos, heterozygous mutant mice show an increase in mitochondrial fission, and impaired optic nerve structure and visual function.[18] *Drp1* gene mutations lead to abnormal brain development, optic atrophy, and neonatal lethality.[19] In addition, dysregulation of Drp1 is related to mitochondrial dysfunction-mediated pain. In the perineural HIV coat glycoprotein gp120-induced neuropathic pain rats, increase of Drp1 expression in spinal cord is observed while antisense oligodeoxynucleotide against Drp1 treatment attenuated mechanical allodynia.[20,21]

Various posttranslational modifications (PTMs) of mitochondrial fission and fusion proteins are involved in the functional regulation of mitochondria.[22] S-palmitoylation is a reversible PTM of specific cysteine residues in proteins with 16-carbon fatty acid palmitate.[23] The process plays important roles in regulation of protein targeting to membranes and is mediated by plamitoyltransferase (PAT).[24] A PAT Zdhhc13 regulates Drp1 S-palmitoylation and mitochondrial fission–fusion process in vitro and in vivo.[25,26] 2-bromopalmitate (2-BP) is an irreversible pan-inhibitor of PATs and has been widely used as a protein palmitoylation inhibitor.[27] It is reported that 2-BP could modulate neuronal differentiation.[28] In this study, we have investigated the effects of 2-BP on BCP rats and examined the mitochondrial fission–fusion process in spinal astrocytes of BCP rats. Our results indicate that 2-BP has an antinociceptive effect in BCP rats via regulating mitochondrial fusion and fission process in spinal astrocytes. The current findings link palmitoylation, astrocytes, and mitochondrial fusion and fission process to the pathogenesis of BCP.

Materials and methods

Cell culture

MRMT-1 rat mammary gland carcinoma cell line was purchased from JENNIO Biological Techonology (Guangzhou, China). MRMT-1 cells were cultured in Roswell Park Memorial Institute (RPMI) 1640 medium (Gibco, MD, USA) containing 10% fetal bovine serum (FBS, heat-inactivated) (Hyclone; Utah, USA), 1% L-glutamine, and 2% penicillin/streptomycin (Gibco, MD, USA). Cells were detached from the flask by 0.25% trypsin for subsequent preparation of injection. Briefly, the cells were collected by centrifugation and the pellet was resuspended in Hank's balance salt solution (HBSS).

C6 glia cells were cultured in RPMI 1640 medium (Gibco, MD, USA) containing 10% FBS (Hyclone; Utah, USA), 50 U/ml penicillin, and 50 mg/ml streptomycin (Gibco, MD, USA). C6 cells were grown in a humidified incubator at 37°C with 5% CO_2. 70%–80% confluent cells were used for 2-BP treatment. The concentration of 2-BP for cell treatment were 1 μM and 10 μM. Control group was incubated with equal volume of dimethyl sulfoxide (DMSO). After 24 h of incubation, the whole-cell extracts from control and 2-BP treated cells were collected for biochemical analysis.

Experimental animals

Female Sprague–Dawley (SD) rats weighing 160 to 200 g were purchased from Hubei Province Experimental Animal Center (Wuhan, China). All animals were house with ad libitum access to water and food in a 12/12 h light–dark cycle regime and environmental temperature was controlled at 22 ± 1°C. Animals were

housed for seven days to acclimatize before the experimental procedures. All experimental procedures in this study were complied with the local and international guidelines on ethical use of animals and all efforts were made to minimize the number of animals used and their sufferings.

Surgical procedure for establishing a rat model of BCP

A rat model of BCP was established following previous reports.[32] Briefly, female SD rats were deeply anesthetized with pentobarbital sodium (50 mg/kg, intraperitoneal injection). The left leg of rat was shaved and the top half of the tibia was carefully exposed after disinfection with 7% iodine and 75% (v/v) ethanol. Subsequently, 3.5×10^5 MRMT-1 cells were slowly injected into the intramedullary space of the left tibia in the rats to establish the BCP model. An equivalent volume of HBSS solution was injected into the sham rats using a 50 µl Hamilton microsyringe. Syringe was left in the injection site for an additional minute to prevent the leakage of tumor cells. Injection site was sealed with bone wax after syringe was removed. Radiological and histological detections were used to evaluate the bone destruction after inoculation of MRMT-1 cells.

Drug administration

Intrathecal injection of 2-BP was used for treatment of BCP rats. Briefly, 2-BP was dissolved in DMSO (Sigma-Aldrich, MO, USA) and then diluted in saline. The dose for intrathecal administration of 2-BP was selected according to previous research[28] and our preliminary studies. When injecting, rats were held firmly, and 25 µl microsyringe was inserted between L5 and L6 vertebrae. A sudden advancement of the needle accompanied by a slight flick of the tail was used as the indicator for the proper insertion into the subarachnoid space.[29] Rats (n = 30) were randomly divided into three groups: Sham group; BCP group; BCP + 2-BP group, each group contained 10 rats. For sham group, rats were intrathecally injected with 10 µl vehicles (DMSO+saline). Rats in BCP group were intrathecally injected with 10 µl vehicles (DMSO + saline). For BCP + 2-BP group, rats were intrathecally injected with 10 µl 2-BP (0.5 mg/kg). 2-BP was injected on 12 days after surgery and after 24 h treatment, the rats were euthanized with an overdose of pentobarbital sodium (100–150 mg/kg) and lumbar spinal cords were separated and collected for morphological and biological analysis.

Radiology

Rats were anesthetized with sodium pentobarbital and exposed to an X-ray source. Roentgenography of the ipsilateral tibia was performed on postoperative day (POD) 12 and POD 20. Radiographs were taken from hind limbs of sham and BCP rats.

Bone and spinal cord histology

On day 12 following inoculation of MRMT-1 cells or HBSS, rats were deeply anesthetized with pentobarbital sodium (50 mg/kg, intraperitoneal injection). After transcardially perfused fixative with 4% paraformaldehyde, tissues were isolated from animals and postfixed in the same fixative for 6 h at 4°C. The left tibial bone was preserved in 10% neutral buffered formalin and decalcified using 10% ethylenediaminetetraacetic for 21 days. Then, the bones were embedded in paraffin and sections were cut into 5 µm (Leica RM 2165) and stained using standard haematoxylin and eosin (H&E) method to visualize the extent of bone destruction. Lumbar spinal cords were then immersed in 20% to 30% (w/v) gradient of sucrose in phosphate-buffered saline (PBS) for 24 h at 4°C, followed by freezing in isopentane (−40°C). Frozen specimens were sectioned at 6 µm with a freezing microtome and stained with H&E to measure the extent of inflammatory infiltration.

Mechanical allodynia

Rats were placed on a 5 × 5 mm wire mesh grid floor and allowed to habituate for 30 min. Test was blinded with respect to group. The von Frey filaments (ranging from 0.4 g to 26 g) (Stoelting, Wood Dale, IL, USA) were used to apply mechanical stimuli to the left hind paw. The 50% paw withdrawal threshold (PWT) was determined by Chaplan's up-down method.[30] Briefly, the calibrated monofilaments were applied perpendicularly to the plantar surfaces until the filaments were bent, and a brisk withdrawal was considered as positive response. Whenever a positive response occurred, the von Frey filament with the next lower force was applied, and whenever a negative response occurred, the filament with the next higher force was applied. Then, the pattern of positive and negative withdrawal responses was converted to 50% PWT.

Western blot

After pain behavioral tests, the rats were anesthetized and sacrificed by decapitation on day 12 after inoculation of MRMT-1 cells. Lumbar spinal cord was dissected and then homogenized in ice-cold radioimmunoprecipitation assay (RIPA) lysis buffer containing a cocktail of protease inhibitors (Sigma). After centrifugation at 12,000 g for 15 min, supernatant was used for Western blot analysis. Protein concentrations were determined by bicinchoninic acid assay method. Equal amounts of protein samples were separated in

10% sodium dodecyl sulfate-polyacrylamide gel electrophoresis. Proteins were transferred onto a polyvinylidene difluoride membrane and then incubated with the appropriate primary antibodies at 4°C overnight. The following antibodies were used in this study and ABclonal Technology (Wuhan, China): mouse rabbit anti-Drp1 (1:1000, A2586), anti-OPA1 (1:1000, A9833), mouse anti-glial fibrillary acidic protein (GFAP) (1:1000, A0014), rabbit anti-caspase 3 (1:1000, A11319), rabbit anti-Bcl-2 (1:1000, A0208), rabbit anti-β-actin (1:5000, AC004). Horse radish peroxidase (HRP)-conjugated secondary antibodies (1:5000, Abcam) were used to visualize the primary antibodies. Infrared Imaging System (Gene Company Limited, Hongkong, China) was applied to detect immunoreactive bands.

Immunofluorescene

Twelve days after surgery, rats were transcardially perfused fixative with 4% paraformaldehyde, and lumbar spinal cords were removed and immersed in 20% to 30% (w/v) gradient of sucrose in PBS for 24 h at 4°C. Frozen spinal sections (6 μm) were cut with a freezing microtome and incubated with 10% normal donkey serum for 1 h at room temperature. Subsequently, the sections were incubated with primary antibody, mouse anti-GFAP antibody (1:50, A0014), overnight at 4°C. After incubation and being washed with PBS, sections were incubated with goat anti-mouse IgG H&L (fluorescein isothiocyanate) (1:200) at room temperature for 1 h and then examined with a fluorescence microscope.

For cells, C6 cells were seeded onto sterilized coverslips which were placed in 24-well plates glass slides for different treatment. After treatment, cells (50∼70% confluent) were fixed with 4% paraformaldehyde and permeabilized with 0.5% Triton X-100 in PBS buffer. After rinsing cells on the coverslips with 0.2% Triton X-100 in PBS, blocking buffer (5% donkey serum) was added and incubated for 60 min. Primary antibodies: rabbit anti-Drp1 (1:100, A2586) and rabbit anti-OPA1 (1:100, A9833) were added and incubated for 24 h at 4°C. After three washes, the cells were incubated with goat anti-rabbit IgG H&L (tetramethylrhodamine isothiocyanate (TRITC)) secondary antibodies (Abcam) at room temperature for 60 min. Subsequently, the cells were washed and counterstained with Hoechst (1 μg/ml) for 15 min and examined with a fluorescence microscope.

Enzyme-linked immunosorbent assay analysis of BAX and IL-1β

IL-1β (Boster, Wuhan, China) and BCL-2-associated x protein (BAX) (Shanghai Haling Biotechnology, Shanghai China) levels in spinal cord lysates were determined using commercially available, enzyme-linked immunosorbent assay (ELISA) kits, according to the manufacturer's protocols.

For IL-1β assay, ipsilateral lumbar spinal cord was homogenized and lysed in ice-cold RIPA buffer pH 7.4 containing a protease inhibitor cocktail. After centrifugation at 12,000 g for 15 min, the supernatant was used for ELISA analysis. According to the manufacturer's protocols, 100 μl tissue lysates and different concentrations of standard reagent were added to a 96-well plate that precoated with rat IL-1β specific antibody and incubated at 37°C for 90 min. After the wells were emptied, 100 μl biotinylated anti-rat IL-1β antibody was added and incubated at 37°C for 60 min. After addition of avidin-biotin-peroxidase-complex for 30 min at 37°C and color development, the reaction was terminated by 3,3′,5,5′-tetramethylbenzidine solution. The absorbance was measured at 450 nm on a microplate reader (BioTek Instruments, INC., USA). IL-1β assay had a linear over a range of 31.2–2000 pg/ml. The intra-assay and inter-assay coefficients of variation for IL-1β are 5.6% and 7.1%.

For BAX assay, ipsilateral lumbar spinal cord was homogenized and lysed in ice-cold PBS buffer pH 7.4 containing a protease inhibitor cocktail. After centrifugation at 3000 g for 20 min, the supernatant was used for ELISA analysis. Tissue lysates and different concentrations of standard reagent were added to a 96-well plate that was precoated with rat BAX specific antibody and incubated at 37°C for 30 min. After the wells were emptied, 50 μl HRP-Conjugate reagent was added to each well and incubated at 37°C for 30 min. After addition of Chromogen solution A and B and color development for 15 min at 37°C, the reaction was terminated by stop solution. The absorbance was measured at 450 nm on a microplate reader (BioTek Instruments, INC., USA). The BAX assay had a linear over a range of 20–800 ng/l. The intra-assay and inter-assay coefficients of variation for BAX are 9% and 15%, respectively.

Mitochondria membrane potentials measurement

JC-1 Mitochondrial Membrane Potential (MPP) Assay Kit was used to evaluate mitochondria membrane potential (MMP) (Beyotime, China). According to the kit instructions, after 2-BP treatment, cells were washed with ice-cold PBS and stained with JC-1 fluorescent probe for 20 min in the dark at 37°C. Subsequently, culture medium was added, and fluorescence was detected using a fluorescence microscope.

Statistical analysis

Comparison of values between different experimental groups was done using one-way analysis of variance with repeated measures followed by Bonferroni post hoc tests. Significance was ascribed for $p < 0.05$. All raw data were presented as mean ± SD, except data of PWT test were showed as mean ± SEM.

Results

Inoculation of MRMT-1 cells in the tibia induces bone destruction

After intratibial inoculation with MRMT-1 rat mammary gland carcinoma cells, pathological changes were validated by tibia radiograph and histological analysis. Tibia radiograph showed that ipsilateral tibia bone had signs of radiolucent lesions close to the injection site on POD 12 of BCP rats. And bone destruction exhibited progressive worsening on POD 20 (Figure 1(a)). In contrast, no radiological changes were observed in sham group. Meanwhile, by day 12 after inoculation, the hematoxylin and eosin (H&E)-stained tibia sections showed bone destruction with medullary bone loss, as well as infiltrating osteolytic lesions on POD 12 (Figure 1(b)). These results indicated that inoculation of MRMT-1 cells induces tibia destruction.

Cancer cell inoculation in tibia induces nociceptive behavior and spinal cord leukocyte infiltration

To assess the chronic pain induced by cancer cell inoculation, pain behavioral change was evaluated and presented by mechanical allodynia of hind paws. PWTs of ipsilateral hind paws in rats were tested on 0, 2, 4, 6, 8, 10, and 12 after surgery (Figure 2(a)). Rats inoculated with cancer cells displayed a significant decreased in PWT to von Frey filaments stimulation on POD 6 to POD 12, indicating increased sensitivity of mechanical stimulation in BCP rats. While PWTs of sham rats showed no difference at all the time points (Figure 2(b)). Meantime, histological changes in spinal cord of BCP rats were detected by H&E staining. And as shown in Figure 2(c)), spinal cord of BCP rats showed increased infiltration of inflammatory cells as compared with sham group.

Intrathecal administration of 2-BP attenuates pain behavior in BCP rats

PWTs represent the changes of mechanical sensitivity in animals after treatment. To determine the effects of 2-BP on bone cancer-induced mechanical allodynia, rats were tested by von Frey filaments after 24 h of intrathecal 2-BP administration. There was no significant difference of the PWTs between the sham rats receiving vehicle or 2-BP, suggesting 2-BP had little effect on mechanical sensitivity of sham rats (Figure 3(a)). In contrast, bone cancer-bearing rats treated with 2-BP exhibited significant decrease in nociceptive behavior at post injection 2 h (vehicle vs. 2-BP: 4.3 ± 1.5 vs. 10.8 ± 1.0, $p < 0.05$), 4 h (vehicle vs. 2-BP: 3.6 ± 1.1 vs. 10.1 ± 0.6, $p < 0.05$), 6 h (vehicle vs. 2-BP: 4.8 ± 1.3 vs. 11.1 ± 1.7, $p < 0.05$) and 8 h (vehicle vs. 2-BP: 5.0 ± 0.9 vs. 11.9 ± 1.4, $p < 0.05$), compared with the cancer-bearing rats treated with vehicle (Figure 3(b)). The result indicated that 2-BP had an anti-nociceptive effect in BCP rats.

2-BP down-regulates spinal astrocytes activation of BCP rats

Increasing evidence showed that spinal astrocytes were involved in the process of pain.[6,31] Therefore, we examined activation of astrocytes in the spinal cord by analyzing GFAP (astrocytic biomarker) expression. On day 12 after tumor cell inoculation, GFAP

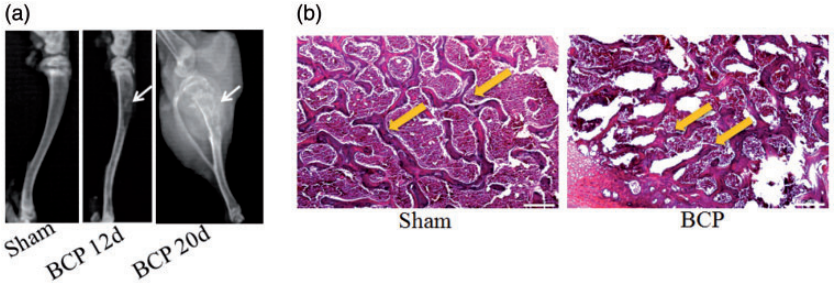

Figure 1. Radiological and histological evaluation of bone destruction after inoculation of MRMT-1 cells. (a) Radiographs of the tibia bone inoculated with MRMT-1 cells 12 and 20 days after inoculation in the ipsilateral hind limbs. Representative radiograph of sham and BCP rats are shown and arrows indicate the position of bone destruction in BCP rats. (b) Histological images of tibia sections stained by hematoxylin–eosin of sham and BCP tibial bone. The sections (5 μm) were taken from tibial bone 12 days after surgery. The arrows in sham group indicate the continuous thick bone trabecular, and the arrows in BCP group show bone destruction on trabecular surface. Scale bar = 200 μm. BCP: bone cancer pain.

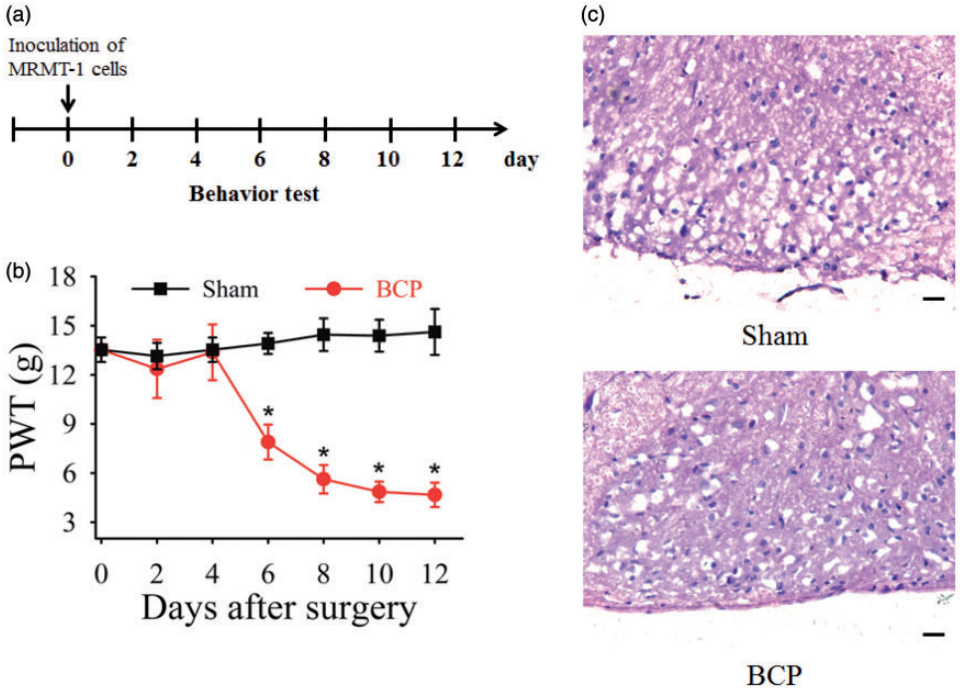

Figure 2. Changes of mechanical response thresholds in sham and BCP rats. (a) Experimental paradigms showing time points of surgery and behavior test. (b) PWTs to von Frey filaments of the ipsilateral paw in sham and BCP rats received intra-tibia inoculations of Hank's buffered sterile saline and MRMT-1 cells, respectively. All data are expressed as the mean ± SEM (n = 9). *$p < 0.05$ vs. sham rats at each corresponding time point. (c) Pathological examination (H&E staining) of spinal cord sections from sham and BCP rats to evaluate inflammation. Scale bar = 100 μm. ■: Sham rats, ○: BCP rats. BCP: bone cancer pain; PWT: paw withdrawal threshold; 2-BP: 2-bromopalmitate.

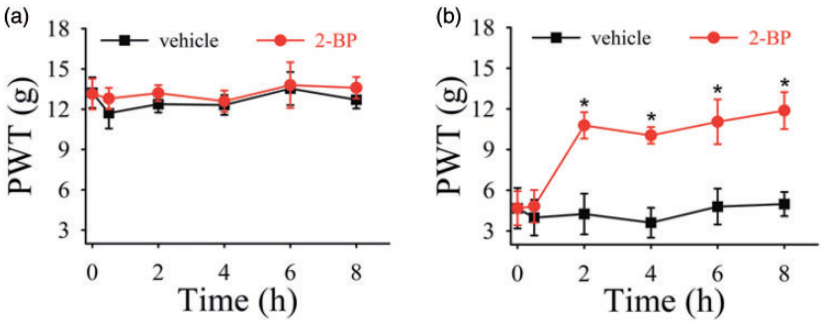

Figure 3. Evaluation of intrathecal administration of 2-BP on PWT in sham and BCP rats. Sham rats (a) and BCP rats (b) were injected with vehicle (DMSO + saline) and 1 mg/kg 2-BP, and the response to von Frey filaments stimulation of mentioned groups were detected. Pain behaviors were analyzed at 0, 2, 4, 6, and 8 h after 2-BP treatment. All data are expressed as the mean ± SEM (n = 9). *$p < 0.05$ vs. vehicle treated rats at each corresponding time point. PWT: paw withdrawal threshold.

immunohistochemistry showed that GFAP-labeled astrocytes in ipsilateral dorsal horn significantly increased in BCP rats, compared with sham rats (Figure 4(a)). This result suggested that bone cancer induced significant astrocytic hyperplasia in the spinal dorsal horn. Subsequently, the expression of GFAP protein was analyzed by Western blotting analysis. Consistent with the increased GFAP staining, we found a significant up-regulation of GFAP protein in BCP rats (Figure 4(b) and (c)). The level of GFAP was markedly decreased in spinal cord of 2-BP treated rats (Figure 4(b) and (c)) which indicated that 2-BP had an effect on resistance of BCP-induced astrocytes activation.

2-BP ameliorates BCP-induced abnormality of mitochondrial dynamics in the spinal cord of BCP rats

Expression of mitochondrial fission- and fusion-related proteins, Drp1 and OPA1, were investigated in various groups to characterize mitochondrial dynamics.

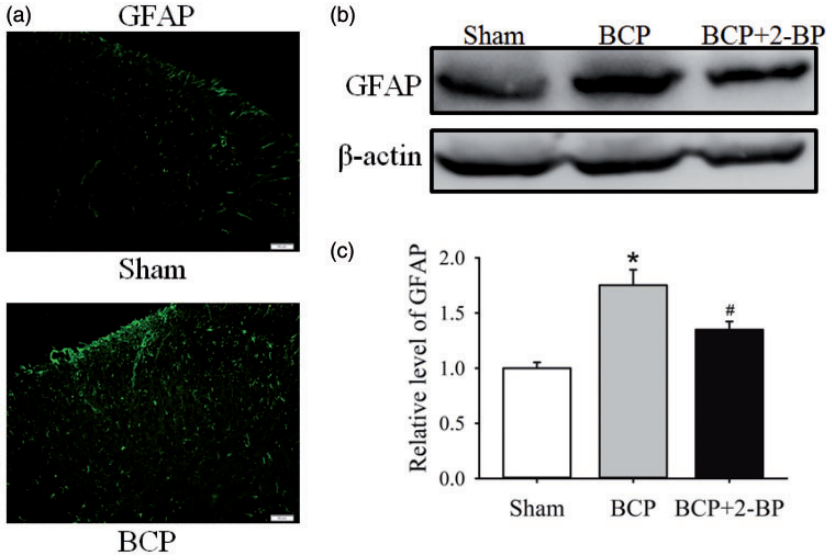

Figure 4. The localization and expression of GFAP in the spinal dorsal horn. (a) Spinal cord sections are stained with GFAP antibody to analyze the distribution of astrocyte marker GFAP in the dorsal horn of sham and BCP rats. Panels represented dorsal horn of sham and BCP rats (n = 6). Scale bar = 50 μm. (b) Western blot analysis of protein extracts from sham-, BCP-, and 2-BP-treated group. Representative bands show the GFAP protein level. (c) Quantitative analysis of GFAP level in (b) and expressed as fold change over sham group. Data are shown as mean ± SD for three independent trials. $^{*}p < 0.05$ compared with sham group, $^{\#}p < 0.05$ compared with BCP group. 2-BP: 2-bromopalmitate; BCP: bone cancer pain; GFAP: glial fibrillary acidic protein.

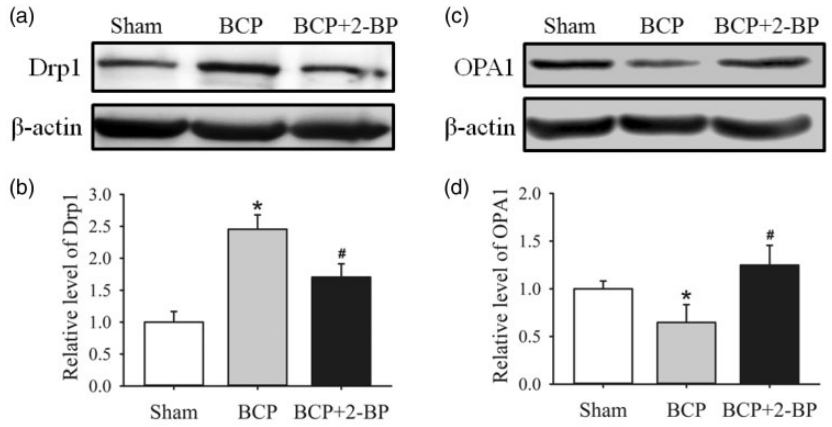

Figure 5. Determination of Drp1 and OPA1 expression in sham, BCP and 2-BP-treated BCP rats. (a and c) Western blot analysis of protein levels of Drp1 and OPA1 in the spinal cord of sham-, BCP-, and 2-BP-treated rats. Representative bands show the Drp1 (a) and OPA1 (c) protein level. (b and d) Quantitative analysis of Drp1 and OPA1 protein level and expressed as fold change over sham group. Data are shown as mean ± SD for three independent trials. $^{*}p < 0.05$ compared with sham group, $^{\#}p < 0.05$ compared with BCP group. 2-BP: 2-bromopalmitate; BCP: bone cancer pain; Drp1: dynamin-related protein 1; OPA1: optic atrophy 1.

Compared with sham rats, expression of Drp1 was significantly higher, while expression of OPA1 was dramatically reduced in spinal cord of BCP rats (Figure 5). Furthermore, to identify whether 2-BP had a resistance effect on BCP-induced abnormality of mitochondrial dynamics, expression of Drp1 and OPA1 in 2-BP treated BCP rats was analyzed. After 24 of 2-BP administration, Drp1 protein expression was reduced while OPA1 protein expression was promoted significantly ($p < 0.05$ vs. BCP, Figure 5). These data indicated that BCP-induced abnormal expression mitochondrial fusion and fission-related proteins was partly reversed by 2-BP.

2-BP reduces proapoptotic factor and proinflammatory cytokines release in BCP rats

Bcl-2 was an inner mitochondrial membrane protein that can block cell death.[32] During apoptosis, BAX was

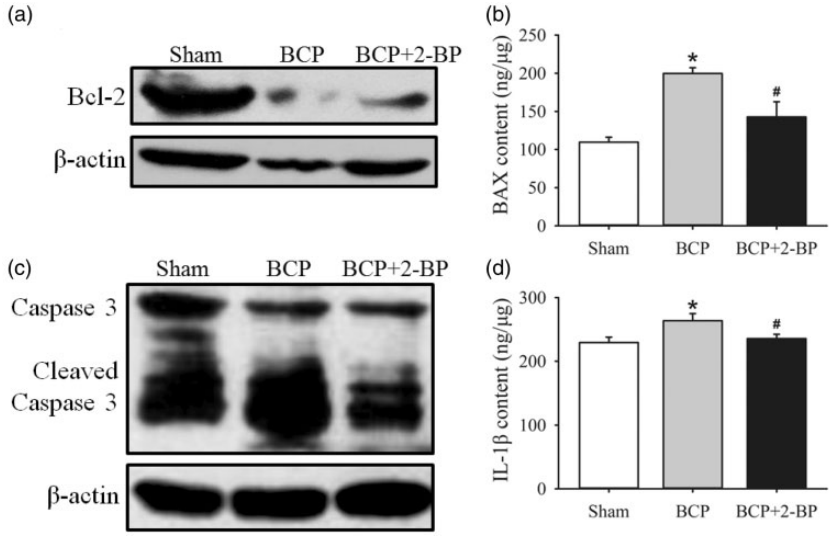

Figure 6. Detection of Bcl-2, caspase 3, BAX, and IL-1β level in various groups. (a and c) Western blot analysis of Bcl-2 and caspase 3 proteins in spinal cord of sham-, BCP-, and 2-BP-treated BCP rats. (b and d) ELISA analysis of BAX and IL-1β protein in spinal cord of sham-, BCP-and 2-BP-treated BCP rats. $^{*}p < 0.05$ vs. sham group, $^{\#}p < 0.05$ vs. BCP group. 2-BP: 2-bromopalmitate; BCP: bone cancer pain.

inserted in MOM which increased permeabilization of MOM and promoted apoptosis.[33] Herein, down-regulation of Bcl-2 content and up-regulation of BAX content was found in spinal cord of BCP rats (Figure 6(a) and (b)). We also detected expression of caspase 3, a mitochondrial apoptosis mediator, which was up-regulated (cleaved caspase 3) in spinal cord of BCP rats (Figure 6(c)). These results suggested that apoptosis in BCP rats was activated. After intrathecal administration of 2-BP, dysregulated Bcl-2, BAX, and caspase 3 expressions were reversed (Figure 6(a) to (c)). Spinal proinflammatory cytokines directly and indirectly induced and exaggerated pain.[34] Activated glia can release proinflammatory cytokines, such as IL-1β.[35] ELISA analysis showed that increased concentration of IL-1β in spinal cord of BCP rats, while 2-BP reversed IL-1β secretion in spinal cord of BCP rats (Figure 4(d)). These data indicated that 2-BP regulated proinflammatory cytokines release and apoptosis in BCP rats.

2-BP regulates mitochondrial fusion and fission dynamic balance in C6 cells

To explore the mechanisms of 2-BP in the regulation of mitochondrial dynamics in astrocytes, C6 rat glioma cells were used in the following experiments. Levels of fusion and fission machinery proteins changes in 2-BP treated C6 cells were assessed. Upon 2-BP treatment, decreased Drp1-fluorescene signal intensity and increased OPA1-fluorescene signal intensity were determined by immunocytochemistry (Figures 7(a) and 8(a)). Consistent with the immunofluorescence staining, Western blot analysis showed that Drp1 protein level was down-regulated and OPA1 protein level was up-regulated after 2-BP treatment, both changes were in a 2-BP dose-dependent manner (Figures 7(b) and 8(b)). The relative level of Drp1 in 1 and 10 μM 2-BP treatment groups was 0.58 ± 0.01 and 0.47 ± 0.09, respectively. The relative level of OPA1 in 1 and 10 μM 2-BP treatment groups was 3.47 ± 0.08 and 4.95 ± 0.25, respectively. These data demonstrated that 2-BP decreased Drp1 expression and increased OPA1 expression in C6 cells.

2-BP increases mitochondrial membrane potential in C6 cells

Change in MMP is closely related to the regulation of apoptosis. JC-1 can selectively enter into mitochondria and reversibly change color from green (the monomeric form of JC-1) to red (the aggregate form of JC-1) as the membrane potential increases.[36] When the mitochondrial MMP is high, JC-1 accumulates in the matrix of the mitochondria to form J-aggregates (Red). When MMP was lost, these aggregates dissipated into monomers (Green) and cells became apoptotic.[37] The fluorescent probe JC-1 was used specifically for analyzing MMP upon 2-BP treatment. As shown in Figure 9, C6 cells treated with 0 and 1 μM 2-BP exhibited red fluorescence, confirming high MMP. As a positive control, C6 cells exposed to carbonyl cyanide 3-chlorophenylhydrazone (CCCP), JC-1 exhibited a green fluorescence with weaken red fluorescence, indicating low MPP. However, when cells were treated with 2-BP for 24 h

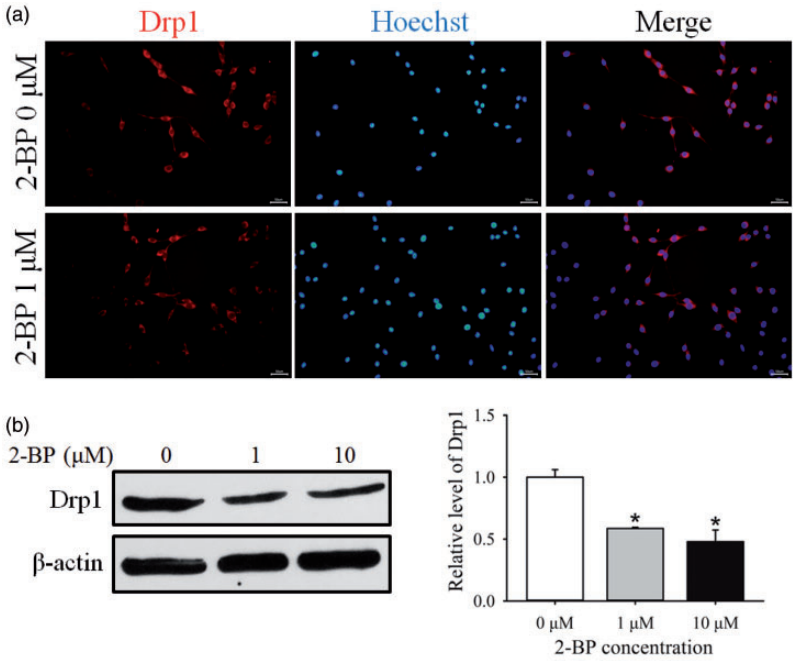

Figure 7. The localization and expression of Drp1 in 2-BP-treated and -untreated C6 cells. (a) After treatment with 2-BP for 24 h, C6 cells were fixed and subjected to immunofluorescence. Anti-Drp1 antibody was probed with anti-rabbit IgG H&L (TRITC) (red). Cells were counterstained with Hoechst 33342 (blue). Scale bar = 50 μm. (b) Western blot analysis of protein extracts from 0, 1, and 10 μM 2-BP-treated C6 cells. Representative bands show the Drp1 protein level. Quantitative analysis of Drp1 protein level, expressed as fold change over 0 μM group. Data were shown as mean ± SD for three independent trials. *$p < 0.05$ compared with 0 μM group. Drp1: dynamin-related protein 1; 2-BP: 2-bromopalmitate.

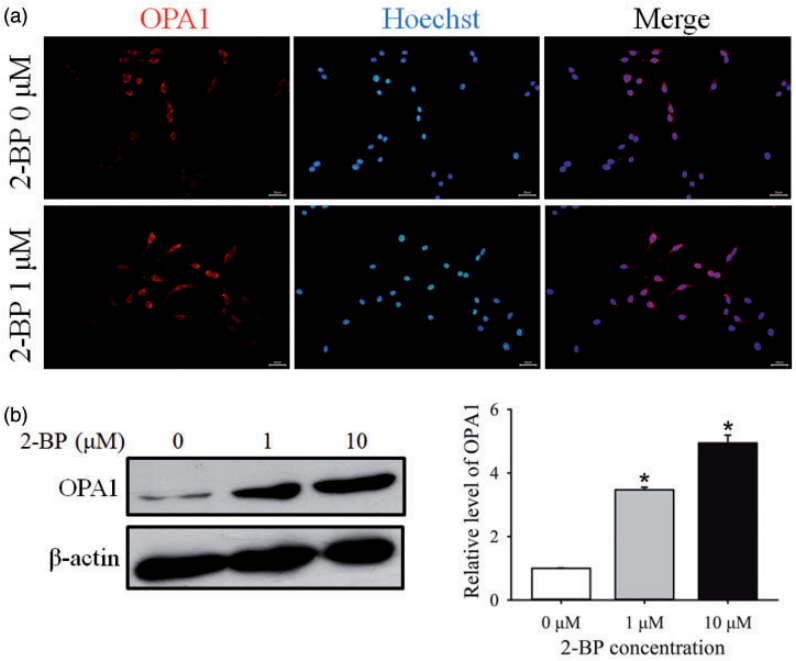

Figure 8. The localization and expression of OPA1 in 2-BP-treated and -untreated C6 cells. (a) After treatment with 2-BP for 24 h, C6 cells were fixed and subjected to immunofluorescence. Anti-OPA1 antibody was probed with anti-rabbit IgG H&L (TRITC) (red). Cells were counterstained with Hoechst 33342 (blue). Scale bar = 50 μm. (b) Western blot analysis of protein extracts from 0, 1, and 10 μM 2-BP treated C6 cells. Representative bands show the OPA1 protein level. Quantitative analysis of OPA1 protein level, expressed as fold change over 0 μM group. Data are shown as mean ± SD for three independent trials. *$p < 0.05$ compared with 0 μM group. 2-BP: 2-bromopalmitate; OPA1: optic atrophy 1.

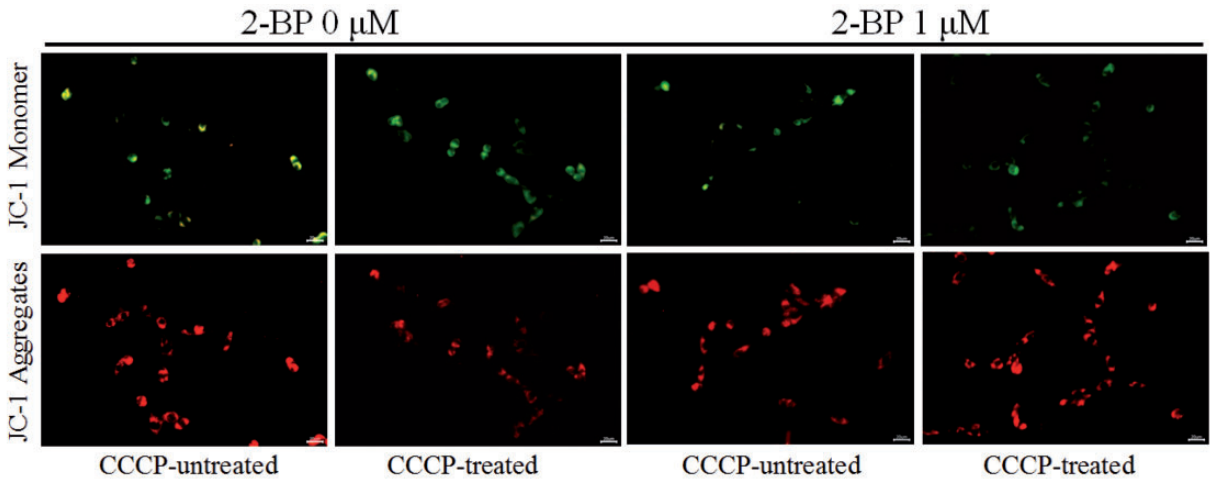

Figure 9. Effect of 2-BP on MMP changes. Representative fluorescent images of JC-1 in untreated and 2-BP-treated C6 cells. CCCP was used as a positive control. Green fluorescence presents monomeric JC-1; Red fluorescence presents aggregate JC-1. Scale bar = 20 μm. 2-BP: 2-bromopalmitate.

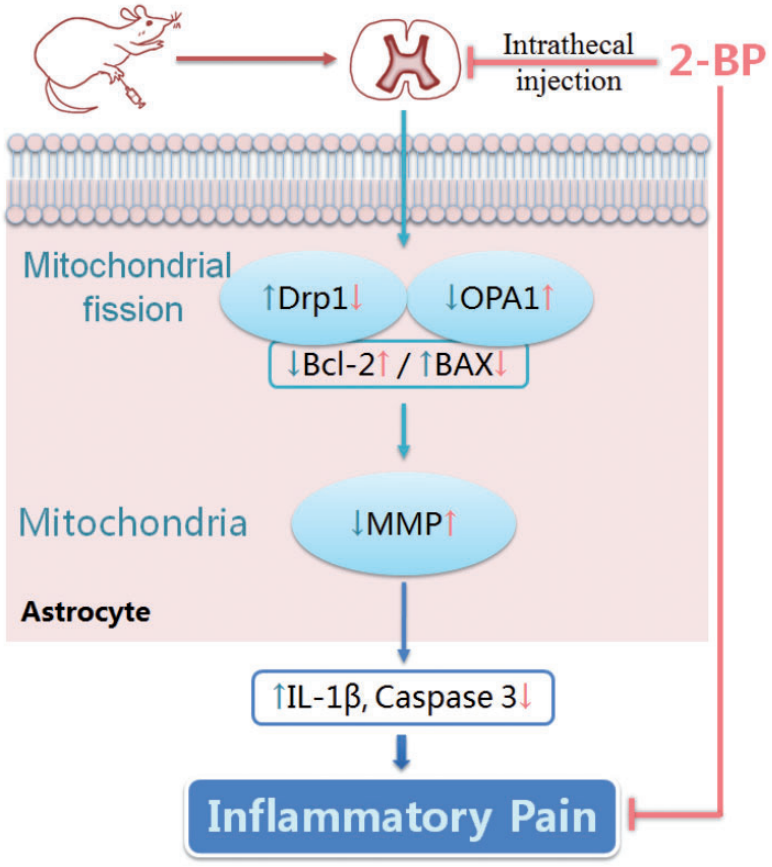

Figure 10. Hypothetical model represents 2-BP attenuates BCP via reversing spinal astrocytic mitochondrial fusion and fission imbalance-induced inflammation and apoptosis. Drp1: dynamin-related protein 1; OPA1: optic atrophy 1.

and then exposed to CCCP, JC-1 still showed high red fluorescence intensity, indicating 2-BP inhibited CCCP-induced decrease in MMP. These data demonstrated that 2-BP reversed CCCP-induced attenuation of MMP.

Discussions

Increasing evidence showed the involvement of protein palmitoylation in regulating mitochondrial functions

which play a vital role in CNS.[22] Palmitoyltransferase Zdhhc13 is important to mitochondrial dynamics, Zdhhc13-deficent mice exhibit lower status of S-palmitoylaton in Drp1-mitochondrial fission-related protein which consequently disrupted mitochondrial dynamics.[26] In addition, immunity-related GTPase (IRG) localized in mitochondria and promoted mitochondrial fission by its residual palmitoylation.[38] 2-BP, the most commonly used inhibitor of palmitoylation, inhibited PAT activity of Asp-His-His-Cys (DHHC) proteins.[23,39] In our study, 2-BP reverses dysregulation of mitochondrial fission-related protein Drp1 induced by BCP. Consistent with the research on animals, 2-BP-treated cells also showed decrease in Drp1 expression. Accordingly, the effect of 2-BP on Drp1 probably linked S-palmitoylation to mitochondrial dynamics.

Abnormal mitochondria were involved in cell death.[40] Before classical signs of apoptosis triggered, mitochondrial membrane integrity underwent major changes, including the dissipated mitochondrial transmembrane potential.[41] We found 2-BP inhibited attenuation of CCCP-induced MPP in C6 cells. Stabilization of mitochondrial membrane could prevent apoptosis. GABAergic interneuron is the main cell type apoptosis in spinal cord. In a mouse model of sciatic nerve injury, loss of GABAergic interneurons in the superficial dorsal horn contributed to the development of neuropathic pain. The reason is the excitotoxic cell death which was mediated by NMDA receptor.[42] In BCP, apoptosis of GABAergic interneuron in the dorsal horn contributed to the development of cancer-induced bone pain.[43] These studies proved that GABAergic interneuron is the critical factor for the development and maintenance of chronic pain. In our study, decreased anti-apoptotic factor Bcl-2, increased proapoptotic factor BAX, and cleaved caspase 3 induced by BCP were reversed by 2-BP treatment. Accordingly, 2-BP probably via suppressing the apoptotic signal in neurons improves the pain behavior of BCP rats. The balance between mitochondrial fusion and fission was important for maintaining mitochondrial morphology and function.[44] In our study, we found up-regulated Drp1 and down-regulated OPA1 in spinal cord of BCP rats, indicating that the balance between fusion and fission was disrupted. The imbalance of mitochondrial dynamics was reversed by 2-BP treatment. Together with above mentioned, 2-BP probably inhibits dysfunction of mitochondrial dynamics and apoptosis via modulating Drp1 protein palmitoylation.

Role of astrocyte during pain pathogenesis has been implicated in several studies.[45–47] Inflammatory activation of astrocytes leads to proinflammatory cytokines expression and neuronal damage. During BCP, inflammatory signal pathway was activated and a lot of inflammatory mediators were released.[48] We found BCP induced increase in marker of astrocytes GFAP expression in spinal cord, and 2-BP treatment decreased GFAP expression. Meanwhile, concentration of IL-1β increased in spinal cord of BCP rats, and 2-BP reversed IL-1β secretion. It was reported that 2-BP had an anti-inflammatory effect by blocking myristoylation and palmitoylation of Fyn (Src family kinases), inhibiting its membrane binding and localization in T-cell signal pathway.[49] Accordingly, 2-BP could be a possible candidate for BCP treatment for its effect on mitochondria-associated inflammatory effect in astrocytes.

Conclusion

Our results demonstrated the inhibitory effect of 2-BP on BCP induced dysregulation of mitochondrial dynamics which consequently attenuates inflammation and apoptosis (Figure 10). The effect could be attributed to the inhibitory action of palmitoylation on Drp1, mediating by 2-BP. The current research provides palmitoylation of Drp1 as a potential target for treatment of BCP.

Declaration of Conflicting Interests

The author(s) declared no potential conflicts of interest with respect to the research, authorship, and/or publication of this article.

Funding

The author(s) disclosed receipt of the following financial support for the research, authorship, and/or publication of this article: This study was financially supported by Research Project of pharmacy key subject (2019-20YZ04, 2018-19XYZ04), Research Project of Hubei Provincial Department of Education (B2018174), and Hubei University of Science and Technology Program (BK201804).

ORCID iD

Min Xie https://orcid.org/0000-0002-0029-0496

References

1. Mantyh P. Bone cancer pain: causes, consequences, and therapeutic opportunities. *Pain* 2013; 154: S54–S62.
2. Mantyh PW. Bone cancer pain: from mechanism to therapy. *Curr Opin Support Palliat Care* 2014; 8: 83–90.
3. De Felice M, Lambert D, Holen I, Escott KJ, Andrew D. Effects of Src-kinase inhibition in cancer-induced bone pain. *Mol Pain* 2016; 12: 1–14.
4. Han MM, Yang CW, Cheung CW, Li J. Blockage of spinal endothelin A receptors attenuates bone cancer pain via regulation of the Akt/ERK signaling pathway in mice. *Neuropeptides* 2018; 68: 36–42.
5. Yang H, Yan H, Li X, Liu J, Cao S, Huang B, Huang D, Wu L. Inhibition of connexin 43 and phosphorylated

NR2B in spinal astrocytes attenuates bone cancer pain in mice. *Front Cell Neurosci* 2018; 12: 129.
6. Song ZP, Xiong BR, Guan XH, Cao F, Manyande A, Zhou YQ, Zheng H, Tian YK. Minocycline attenuates bone cancer pain in rats by inhibiting NF-kappaB in spinal astrocytes. *Acta Pharmacol Sin* 2016; 37: 753–762.
7. Yao Y, Huang JZ, Chen Y, Hu HJ, Tang X, Li X. Effects and mechanism of amyloid beta1-42 on mitochondria in astrocytes. *Mol Med Rep* 2018; 17: 6997–7004.
8. Gao YJ, Ji RR. Targeting astrocyte signaling for chronic pain. *Neurotherapeutics* 2010; 7: 482–493.
9. Hansen RR, Malcangio M. Astrocytes–multitaskers in chronic pain. *Eur J Pharmacol* 2013; 716: 120–128.
10. Chen G, Luo X, Qadri MY, Berta T, Ji RR. Sex-dependent glial signaling in pathological pain: distinct roles of spinal microglia and astrocytes. *Neurosci Bull* 2018; 34: 98–108.
11. Qiu L, Luo Y, Chen X. Quercetin attenuates mitochondrial dysfunction and biogenesis via upregulated AMPK/SIRT1 signaling pathway in OA rats. *Biomed Pharmacother* 2018; 103: 1585–1591.
12. Hayakawa K, Esposito E, Wang X, Terasaki Y, Liu Y, Xing C, Ji X, Lo EH. Transfer of mitochondria from astrocytes to neurons after stroke. *Nature* 2016; 535: 551–555.
13. Serasinghe MN, Chipuk JE. Mitochondrial fission in human diseases. *Handb Exp Pharmacol* 2017; 240: 159–188.
14. Song J, Lei X, Jiao W, Song Y, Chen W, Li J, Chen Z. Effect of Qiangji Jianli decoction on mitochondrial respiratory chain activity and expression of mitochondrial fusion and fission proteins in myasthenia gravis rats. *Sci Rep* 2018; 8: 8623.
15. Chodkowski M, Serafińska I, Brzezicka J, Golke A, Słońska A, Krzyżowska M, Orłowski P, Bąska P, Bańbura MW, Cymerys J. Human herpesvirus type 1 and type 2 disrupt mitochondrial dynamics in human keratinocytes. *Arch Virol* 2018; 163: 2663–2673.
16. Xi Y, Feng D, Tao K, Wang R, Shi Y, Qin H, Murphy MP, Yang Q, Zhao G. MitoQ protects dopaminergic neurons in a 6-OHDA induced PD model by enhancing Mfn2-dependent mitochondrial fusion via activation of PGC-1alpha. *Biochim Biophys Acta Mol Basis Dis* 2018; 1864: 2859–2870.
17. Garcia I, Innis-Whitehouse W, Lopez A, Keniry M, Gilkerson R. Oxidative insults disrupt OPA1-mediated mitochondrial dynamics in cultured mammalian cells. *Redox Rep* 2018; 23: 160–167.
18. Davies VJ, Hollins AJ, Piechota MJ, Yip W, Davies JR, White KE, Nicols PP, Boulton ME, Votruba M. Opa1 deficiency in a mouse model of autosomal dominant optic atrophy impairs mitochondrial morphology, optic nerve structure and visual function. *Hum Mol Genet* 2007; 16: 1307–1318.
19. Waterham HR, Koster J, van Roermund CW, Mooyer PA, Wanders RJ, Leonard JV. A lethal defect of mitochondrial and peroxisomal fission. *N Engl J Med* 2007; 356: 1736–1741.
20. Kanda H, Liu S, Iida T, Yi H, Huang W, Levitt RC, Lubarsky DA, Candiotti KA, Hao S. Inhibition of mitochondrial fission protein reduced mechanical allodynia and suppressed spinal mitochondrial superoxide induced by perineural human immunodeficiency virus gp120 in rats. *Anesth Analg* 2016; 122: 264–272.
21. Ferrari LF, Chum A, Bogen O, Reichling DB, Levine JD. Role of Drp1, a key mitochondrial fission protein, in neuropathic pain. *J Neurosci* 2011; 31: 11404–11410.
22. Tang M, Lu L, Huang Z, Chen L. Palmitoylation signaling: a novel mechanism of mitochondria dynamics and diverse pathologies. *Acta Biochim Biophys Sin (Shanghai)* 2018; 50: 831–833.
23. Aicart-Ramos C, Valero RA, Rodriguez-Crespo I. Protein palmitoylation and subcellular trafficking. *Biochim Biophys Acta* 2011; 1808: 2981–2994.
24. Chen X, Du Z, Shi W, Wang C, Yang Y, Wang F, Yao Y, He K, Hao A. 2-Bromopalmitate modulates neuronal differentiation through the regulation of histone acetylation. *Stem Cell Res* 2014; 12: 481–491.
25. Napoli E, Song G, Liu S, Espejo A, Perez CJ, Benavides F, Giulivi C. Zdhhc13-dependent Drp1 S-palmitoylation impacts brain bioenergetics, anxiety, coordination and motor skills. *Sci Rep* 2017; 7: 12796.
26. Shen L-F, Chen Y-J, Liu K-M, Haddad A N S, Song I-W, Roan H-Y, Chen L-Y, Yen JJY, Chen Y-J, Wu J-Y, Chen Y-T. Role of S-Palmitoylation by ZDHHC13 in mitochondrial function and metabolism in liver. *Sci Rep* 2017; 7: 2182.
27. Zheng B, DeRan M, Li X, Liao X, Fukata M, Wu X. 2-Bromopalmitate analogues as activity-based probes to explore palmitoyl acyltransferases. *J Am Chem Soc* 2013; 135: 7082–7085.
28. Xia T, Cui Y, Shi H, Ma Z, Gu X. The effect of NR2B subunit palmitoylation at the spinal level after chronic dorsal root ganglia compression in rats. *Anesth Analg* 2014; 119: 1208–1214.
29. Wang XT, Zheng R, Suo ZW, Liu YN, Zhang ZY, Ma ZA, Xue Y, Xue M, Yang X, Hu XD. Activity-dependent dephosphorylation of paxillin contributed to nociceptive plasticity in spinal cord dorsal horn. *Pain* 2016; 157: 652–665.
30. Dixon WJ. Efficient analysis of experimental observations. *Annu Rev Pharmacol Toxicol* 1980; 20: 441–462.
31. Ren BX, Gu XP, Zheng YG, Liu CL, Wang D, Sun YE, Ma ZL. Intrathecal injection of metabotropic glutamate receptor subtype 3 and 5 agonist/antagonist attenuates bone cancer pain by inhibition of spinal astrocyte activation in a mouse model. *Anesthesiology* 2012; 116: 122–132.
32. Gross A, McDonnell JM, Korsmeyer SJ. BCL-2 family members and the mitochondria in apoptosis. *Genes Dev* 1999; 13: 1899–1911.
33. Edlich F, Banerjee S, Suzuki M, Cleland MM, Arnoult D, Wang C, Neutzner A, Tjandra N, Youle RJ. Bcl-x(L) retrotranslocates Bax from the mitochondria into the cytosol. *Cell* 2011; 145: 104–116.
34. Watkins LR, Maier SF. The pain of being sick: implications of immune-to-brain communication for understanding pain. *Annu Rev Psychol* 2000; 51: 29–57.
35. Watkins LR, Milligan ED, Maier SF. Glial activation: a driving force for pathological pain. *Trends Neurosci* 2001; 24: 450–455.
36. Smiley ST, Reers M, Mottola-Hartshorn C, Lin M, Chen A, Smith TW, Steele GD Jr, Chen LB. Intracellular

heterogeneity in mitochondrial membrane potentials revealed by a J-aggregate-forming lipophilic cation JC-1. *Proc Natl Acad Sci U S A* 1991; 88: 3671–3675.
37. Bortner CD, Cidlowski JA. Caspase independent/dependent regulation of K(+), cell shrinkage, and mitochondrial membrane potential during lymphocyte apoptosis. *J Biol Chem* 1999; 274: 21953–21962.
38. Henry SC, Schmidt EA, Fessler MB, Taylor GA. Palmitoylation of the immunity related GTPase, Irgm1: impact on membrane localization and ability to promote mitochondrial fission. *PLoS One* 2014; 9: e95021.
39. Jennings BC, Nadolski MJ, Ling Y, Baker MB, Harrison ML, Deschenes RJ, Linder ME. 2-Bromopalmitate and 2-(2-hydroxy-5-nitro-benzylidene)-benzo[b]thiophen-3-one inhibit DHHC-mediated palmitoylation in vitro. *J Lipid Res* 2009; 50: 233–242.
40. Susin SA, Zamzami N, Kroemer G. Mitochondria as regulators of apoptosis: doubt no more. *Biochim Biophys Acta* 1998; 1366: 151–165.
41. de Pablo MA, Susin SA, Jacotot E, Larochette N, Costantini P, Ravagnan L, Zamzami N, Kroemer G. Palmitate induces apoptosis via a direct effect on mitochondria. *Apoptosis* 1999; 4: 81–87.
42. Inquimbert P, Moll M, Latremoliere A, Tong CK, Whang J, Sheehan GF, Smith BM, Korb E, Athie MCP, Babaniyi O, Ghasemlou N, Yanagawa Y, Allis CD, Hof PR, Scholz J. NMDA receptor activation underlies the loss of spinal dorsal horn neurons and the transition to persistent pain after peripheral nerve injury. *Cell Rep* 2018; 23: 2678–2689.
43. Fu Q, Shi D, Zhou Y, Zheng H, Xiang H, Tian X, Gao F, Manyande A, Cao F, Tian Y, Ye D. MHC-I promotes apoptosis of GABAergic interneurons in the spinal dorsal horn and contributes to cancer induced bone pain. *Exp Neurol* 2016; 286: 12–20.
44. Youle RJ, Karbowski M. Mitochondrial fission in apoptosis. *Nat Rev Mol Cell Biol* 2005; 6: 657–663.
45. Lin SX, Lisi L, Dello Russo C, Polak PE, Sharp A, Weinberg G, Kalinin S, Feinstein DL. The anti-inflammatory effects of dimethyl fumarate in astrocytes involve glutathione and haem oxygenase-1. *ASN Neuro* 2011; 3. DOI: 10.1042/AN20100033.
46. Lindia JA, McGowan E, Jochnowitz N, Abbadie C. Induction of CX3CL1 expression in astrocytes and CX3CR1 in microglia in the spinal cord of a rat model of neuropathic pain. *J Pain* 2005; 6: 434–438.
47. Jiang W, Wang Y, Sun W, Zhang M. Morin suppresses astrocyte activation and regulates cytokine release in bone cancer pain rat models. *Phytother Res* 2017; 31: 1298–1304.
48. Lozano-Ondoua AN, Symons-Liguori AM, Vanderah TW. Cancer-induced bone pain: mechanisms and models. *Neurosci Lett* 2013; 557 PtA: 52–59.
49. Webb Y, Hermida-Matsumoto L, Resh MD. Inhibition of protein palmitoylation, raft localization, and T cell signaling by 2-bromopalmitate and polyunsaturated fatty acids. *J Biol Chem* 2000; 275: 261–270.